



NLR-TP-2005-518

Measured states of Slososat FLEVO

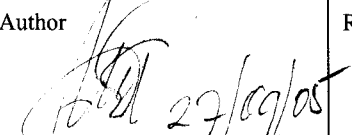
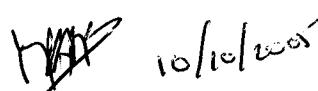
J.P.B. Vreeburg

This report has been based on a paper presented at IAF Congress, Fukuoka, Japan, 17-21 October, 2005.

This report may be cited on condition that full credit is given to NLR and the author.

Customer: National Aerospace Laboratory NLR
Working Plan number: R.1.C.3, R.2.C.1, R.2.C.4
Owner: National Aerospace Laboratory NLR
Division: Aerospace Systems & Applications
Distribution: Unlimited
Classification title: Unclassified
September 2005

Approved by:

Author	Reviewer	Managing department
		



Summary

Sloshsat FLEVO is a spacecraft for the experimental study of liquid dynamics and liquid management problems in space. It was launched in GTO as part of the test payload of Ariane 5 ECA on 12 February 2005. Of the total 129 kg mass of Sloshsat, 33.5 kg is liquid water in a smooth 87 litre tank. The operation of Sloshsat is controlled with an orthogonal set of 12 nitrogen gas thrusters of 0.785 N each. The response of Sloshsat to the control thrusts is predicted from the Sloshsat Motion Simulator (SMS). Sloshsat FLEVO is instrumented with six linear accelerometers and three gyroscopes. The data from these sensors allow to determine the motion of the tank. Since the inertial properties of the empty Sloshsat are known, the force and torque on the tank can be calculated. Over a period of 8 days, Sloshsat has been operated during about 57 hours. Thruster activations have been performed ranging from perturbation pulses to manoeuvres under closed-loop control, from initial conditions at rest or spinning. Discussed now is the behaviour of Sloshsat FLEVO from measured states limited to Weber numbers larger than about 2. Special attention is given to the liquid centre of mass location and the liquid response to control actions. Conclusions on the observed motions and damping behaviour have been formulated, supported by predictions from SMS, in particular for a flat-spin manoeuvre. The friction mechanisms may need to be supplied with others. The Sloshsat Investigators' Working Group is introduced, and the near real-time communication link by internet (FACT).



Contents

1	Introduction	5
2	Background	5
3	Spacecraft Properties	6
4	Science team and operations	7
5	Experiments and data record	8
6	Hydrostatics and accelerometer bias	10
7	The liquid interaction with the tank	13
8	Sloshsat dynamic state	14
9	The Sloshsat Motion Simulator	17
10	Sloshsat/SMS flat-spin manoeuvre	18
11	Conclusions	21
	Nomenclature	22
	References	24

(24 pages in total)



1 Introduction

Various space missions require a vehicle with manoeuvring capability. Examples are: planetary landers, upper stages with restart capability and spacecraft that need to evade hostile action. Other vehicles perform manoeuvres very slowly and can be fitted with electric propulsion, but the listed examples generally contain liquid fuel that represents a considerable fraction of their total mass. Refuelling is often an attractive option and requires tanker spacecraft and RendezVous and Docking (RVD) operations.

Spacecraft control methods require a dynamic model of the system that is used to determine the actuator commands for the achievement of the desired manoeuvre. Such model also serves in simulations to identify manoeuvres or to determine optimal actuation strategies. A wide range of models has been discussed in the literature, from heuristic 2nd-order oscillators to Computational Fluid Dynamics (CFD) formulations with many thousands of cells. A major objective of the Sloshsat FLEVO mission has been the validation of models that predict the behaviour of a spacecraft with a large tank partially filled with liquid. Of particular interest is the model in the Sloshsat Motion Simulator (SMS) that was used to prepare the Experiment Definition Document and the flight operations. The model is of the type that supports a flight mechanics of spacecraft with liquid, i.e. the predicted inertial parameters and dynamic variables correspond to real, measurable physical quantities. In distinction with CFD models, only quantities integrated over the liquid volume are included in the model state, leading to a small number of variables and potential application in onboard logic.

The presented results are based on Sloshsat data that have not yet been corrected for various errors. A major objective now is to show the methods of analysis and the algorithms used. Sloshsat manoeuvres at capillary-dominated, or low Weber number, conditions have not been considered.

2 Background

Slosh dynamics of spacecraft has been researched at NLR since thirty years [1]. Experiments have been performed in the Spacelab Fluid Physics Module, during parabolic flight and with the Wet Satellite Model launched on the MASER 5 sounding rocket. The Sloshsat proposal was submitted to ESA in 1989, in response to an Announcement of Opportunity for the Technology Demonstration Programme (see also [2]). Accommodation as a HitchHiker payload was agreed with NASA in exchange for part of the experiment time and some communication hardware. In the end no flight opportunity materialized, and Sloshsat FLEVO was qualified for launch on Ariane 5 as part of the Maqsat test article. Ariane 5-ECA put Sloshsat in GTO on 12 February

2005. The spacecraft was operated from the Diane ground station in Kourou French Guyana, until all propulsion gas was exhausted on February 21, for a total 57.5 hours of data [3].

3 Spacecraft Properties

A picture of Sloshsat is given as Figure 1.



Figure 1 Sloshsat FLEVO on top of Maqsat.

A wire frame with scaled dimensions, including the tank shape and the locations of the 12 gaseous nitrogen thrusters (0.785 N each) is shown in Figure 2. The water content is indicated by a multi-colour ball.

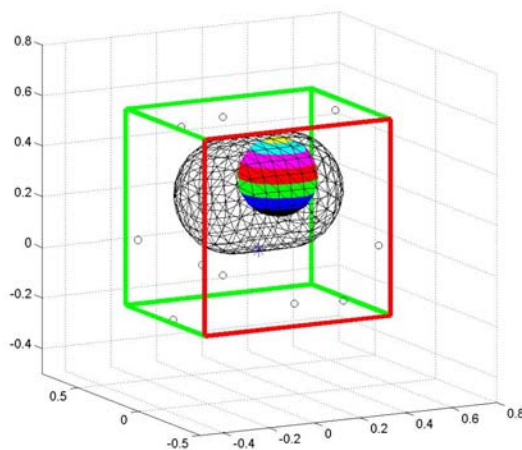


Figure 2 Outline of the main Sloshsat features.



The dry Sloshsat inertial properties are: mass 95.6 kg, centre of mass location [0.0208 -0.0016 -0.2201] m, principal inertia tensor [8.542 -0.065 0.136 -0.065 10.767 -0.198 0.136 -0.198 8.727] kg.m².

The measures are in the coordinate system depicted in Figure 2, centred at the geometric centre (TGC) of the tank. The tank radius is 0.228, its shape has two hemispherical ends separated by a cylindrical surface of length equal to radius. The tank axis is along the X-axis of the frame. The water mass is 33.5 kg.

The inertial properties had been determined accurately but additional structure was added to qualify for Ariane 5 launch. Corrections were made by computation and will be reviewed when Sloshsat data have been corrected finally.

The Sloshsat tank is made of polyethylene and is enclosed in a metal container of conforming size. The spacing between tank and container is about 2 cm and houses the electronics for the tank instrumentation. It includes a capacitive liquid sensing system, the Coarse Sensor Array, and ten thermal anemometers for liquid flow [4]. Data are collected by the On Board Computer (OBC) on the spacecraft platform. The OBC also receives the data from the Motion Sensing Subsystem (MSS) that samples three Litef μ FORS 36/6 fibre optic gyroscopes and six Allied Signal QA-3000-010 accelerometers at 30 Hz. The accelerometers are in three pairs at corners in the Sloshsat structure, i.e. they record accelerations from angular rate in addition to translational motion. Their output is passed through a high-frequency filter with cut-off at about 3 Hz.

The thruster subsystem [5] is activated at 30 Hz. The commands are part of the telemetry, as are the low pressure data that determine the actually delivered thrust. Housekeeping data include temperature measurements at many locations and allow correcting instrument data for thermal effects.

4 Science team and operations

The Sloshsat Investigators' Working Group (IWG) is composed of academic researchers from Groningen State University (NL), Delft Technical University (NL), Technion (Israel), and investigators from ESA, NASA and NLR. They provided input for the Experiment Definition Document (EDD) and participated in the actual operations via the so-called Flight-demonstrator Advanced Crew Terminal (FACT) a project carried out by NLR and Atos Origin (NL). The major project goal is to create a data distribution and operations support tool for the Sloshsat FLEVO satellite telemetry based on generic software.

The IWG members have been supplied with the FACT software that allow them to receive processed Sloshsat telemetry in near-realtime, the same data as used by the operations team at



the Diane ground station. Consultations between investigators at their home base and this team were conducted via internet also.

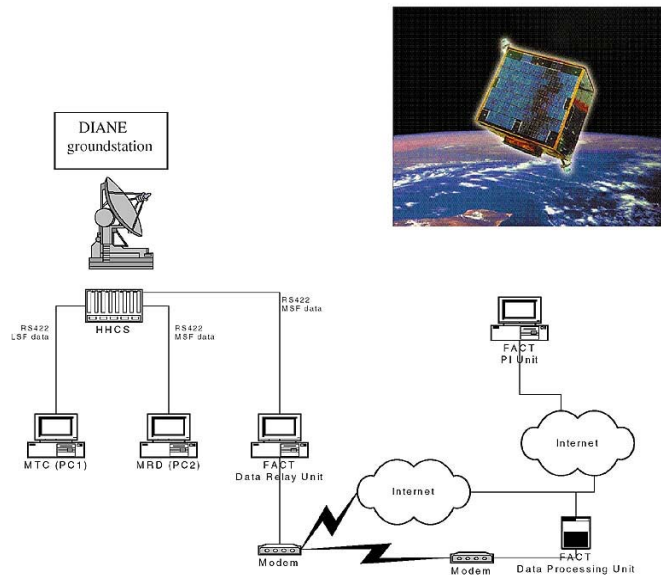


Figure 3 FACT architecture.

5 Experiments and data record

The experiment categories in the EDD [6] are firstly organized in small and large motions. The operations are described as manoeuvres according to:

pulse = short-duration activation of 1 or 2 thrusters

MAX2INT = commanded rotation of the Sloshsat spin vector about a specified point (water c.o.m.)

CONTR10 = PI-control to specified rotation rate (for damping and spin-up/down)

NAM = Nutation Avoidance Manoeuvre (3 timed pulses in sequence)

LTM = translation manoeuvre along the tank axis

The typical large manoeuvre MAX2INT takes Sloshsat from its stable spin about the major axis to a rotation about the intermediate axis. Then thruster activation stops and the ensuing transfer of Sloshsat to stable spin is recorded. 'Spin-over in a partially filled vessel' is a general description of the liquid flow [1]; 'rimming flow' also has some bearing. 'Kneading' of the water by the variable confinement in inertial space is to be modelled. The momentum exchange can be very efficient, or friction high, illustrated by the liquid-filled 'Kelvin top' or the spacecraft liquid phenomenon known as 'anomalous resonance'.



The sum total of all pass durations is about 57h 30m, over an 8 day period. Details are in Table I; the times hrs:min:sec are in Spacecraft Elapsed Time (SET).

Table 1 Data record of the Sloshsat FLEVO mission

Pass #	final	initial	manoeuvres
01	020:23:25	011:28:26	pulse, MAX2INT
02	041:08:40	032:31:28	NAM, CONTR10, pulse
03	061:40:20	058:05:07	pulse, LTM
04	067:49:36	064:09:05	MAX2INT, CONTR10
05	073:27:58	073:12:51	PERIGEE pass data
06	093:14:33	085:06:17	MAX2INT, CONTR10, NAM
07	115:19:53	106:15:31	NAM, eigenf, CONTR10, MAX2INT, LTM, pulse
08	135:53:20	127:34:30	pulse, CONTR10, LTM
09	164:59:20	158:53:30	LTM, pulse, blowdown
10	207:47:30	206:01:33	calibration, valve actions

The major mission anomaly was discovered at the first acquisition of signal in the Diane ground station. Sloshsat telemetry data did not contain any information from inside the experiment container. Thence there are no measurements from the Coarse Sensor Array on liquid distribution, or from the ten thermal anemometers that give local water speed. All scientific data processing has to be limited to the MSS data records. These data appear to be of high quality. A specific item during assessment of flight results is whether there could have been water leaking from the tank and cause electronic malfunction. It is assumed that in that case the inertial properties of the system will be modified also. The effect is small and will therefore be more apparent at a later stage of the flight evaluation, when more precise data will have been generated.

Another anomaly has been leakage of nitrogen gas from the thruster subsystem. It put constraints on the timing of the operations since the opening of one (of the four) pressure vessel marks the start of a finite period of controlled experiments. In addition the leak causes force and torque of unknown magnitude and direction on the system.

During the final Pass Sloshsat was without nitrogen gas and at very low spin. The MSS data are used to determine a first value for the accelerometer bias. Thruster activation has been commanded to determine the effect of valve ringing on the accelerometer output. Precise correction of the raw data for thermal effects and various error sources is necessary and planned, but the evaluations in the next sections are presented already. It is assessed that for the aspects discussed only irrelevant changes are brought by better data and that speedy dissemination of results is more important.



6 Hydrostatics and accelerometer bias

The hydrostatic configuration is characterized by the ratio between pressures from inertial effects (angular rate) and from surface tension. For the conditions in Sloshsat the rotational Weber number $We = 165 \Omega^2$. For $We \gg 1$, the influence of surface tension can be neglected. At the beginning of each Pass Sloshsat was found with uniform spin, i.e. in hydrostatic equilibrium. There is no cause to distrust the gyroscope data and these will be taken as correct. Rotation rate values averaged over two minutes at a time early in the Pass are in Table II:

Table II. Initial spin rate of Sloshsat, $tw0(x,y,z)$ in 1/s

Pass	tw0(1)	tw0(2)	tw0(3)
01	-0.0036	0.1040	-0.0072
02	0.0033	-0.1009	0.0069
03	0.0002	0.0049	-0.0007
04	0.0036	-0.1116	0.0078
05	-0.0048	0.1428	-0.0100
06	-0.0054	0.1613	-0.0112
07	0.0215	-0.6160	0.0435
08	-0.0006	0.0178	-0.0016
09	0.0009	0.0090	-0.0025
10	-0.0004	0.0057	-0.0005

Since the major axis of Sloshsat is nearly coincident with the Y-axis, $tw0(2)$ gives a good indication of the magnitude of spin. Of the other components, $tw0(1)$ is $O(0.5*tw0(3))$, except at the very low values i.e. at low Weber numbers.

The spin axis in Pass 07, with the largest spin value, is in direction $[-0.0348, 0.9969, -0.0704]$. In absence of torque it is also the direction of the major system axis of inertia. The same property, calculated by CFD programme ComFlo [7] at 5 rpm is: $[-0.0282, 0.9979, -0.0588]$. If the meniscus shape is known, the inertial properties can be calculated by direct integration, and iterated to the equilibrium conditions. For a flat surface normal to the centrifugal acceleration, the major axis direction comes out: $[-0.0311, 0.9981, -0.0528]$.

Other results of this calculation are:

water c.o.m. location: $[-0.0263, 0.0021, 0.1101]$ m

system principal inertia tensor: $\begin{bmatrix} 11.6884 & -0.0619 & 0.4575 \\ -0.0619 & 14.4338 & -0.2232 \\ 0.4575 & -0.2232 & 9.9598 \end{bmatrix}$ kg.m².

A cylindrical or spherical free surface is likely to result in somewhat different values.



The magnitude of the effect of gas leakage torque can be estimated. Pass 5 is the perigee pass at SET 073:12:51. Its equilibrium rate was established since the end of Pass 4 at about SET 068, and was modified only by the disturbance torque from gas leakage until Pass 6 initiation at about SET 085.

The average spin acceleration (over 12h 38m 40s) is $0.406 \cdot 10^{-6} \text{ 1/s}^2$, or per hour a spin increase of 0.0015 1/s , i.e. $0.1^\circ/\text{s}$, and makes for a leakage torque of $0(6 \cdot 10^{-6} \text{ N.m})$. If the torque is not aligned with the spin axis, a likely situation, viscous dissipation will still cause the spin to increase and so represent the added system kinetic energy from work by the leakage torque. Although the recorded gas low pressure at about 11 bar is below the nominal value, it is still sufficient to allow a valid torque estimate.

The leakage force is also low; if it were large while the torque is low it would need to pass unbelievably close to the system c.o.m.: for a force 0.06 N, i.e. of capillary magnitude, the arm would need to be 10^{-4} m . Therefore is concluded that the gas leakage effect is insignificant for the Sloshsat dynamics. Whether gas leakage torque is responsible for the aberrant ratio $tw0(1)/tw0(3)$ at low We remains to be analysed, as is a possible effect on hydrostatic diagnosis. The hydrostatic configuration at Pass 10 is nominally steady and thereby serves as a constant condition for the MSS accelerometer output. The smoothed Sloshsat angular rate magnitude has been plotted in Figure 4.

The rate increase over an hour, about $0.005^\circ/\text{s}$, is negligible in comparison with that found from Pass 5. If the rate increase results from torque, i.e. from water vapour that escapes from the container, the magnitude is very small.

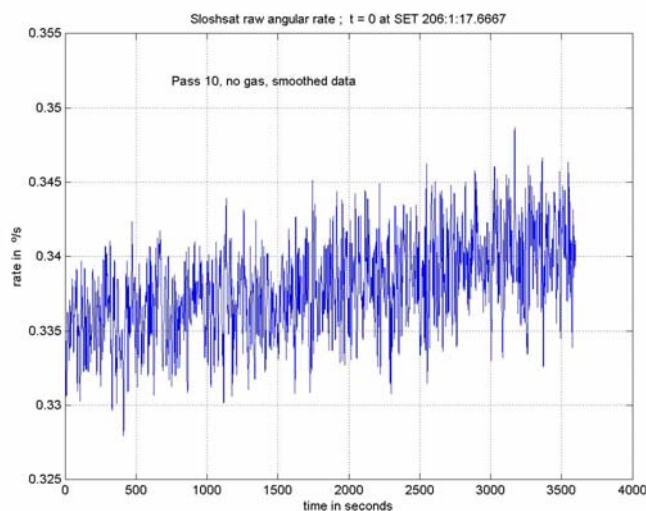


Figure 4 The Sloshsat angular rate magnitude after all gas had been exhausted.

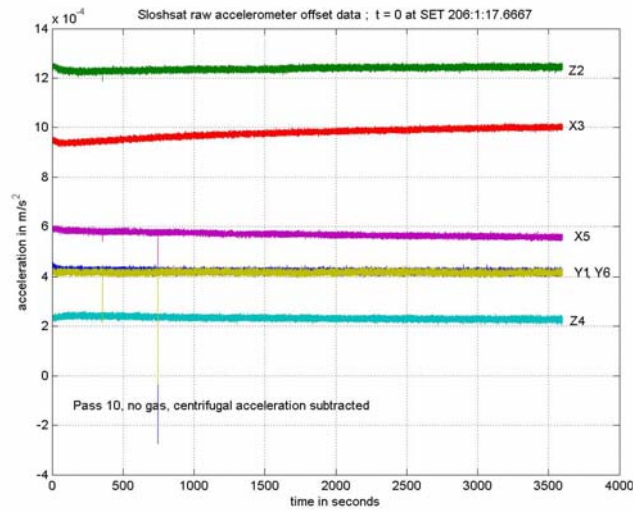


Figure 5 The raw accelerometer offset data in Pass 10.

The accelerometer data are plotted in one figure. The curves in Figure 5 (and Figure 4) are typical for the drift of the bias from temperature change (resulting from system switch on). The contribution from centrifugal acceleration is $O(10^{-5} \text{ m/s}^2)$, i.e. is negligible.

The observed signal is taken to represent offset, or bias. It is remarkable that all values are positive, cause to investigate the gyro calibration. The averaged bias values for the accelerometers are:

Y1	Z2	X3	Z4	X5	Y6
0.42	1.23	0.98	0.24	0.57	0.42

where the accelerometer identification is in the first row, above the bias acceleration in 10^{-3} m/s^2 .

The Allied Signal QA-3000-010 accelerometers of Sloshsat have their Composite Repeatability quoted as $180 \mu\text{g}$, or $1.8 * 10^{-3} \text{ m/s}^2$, larger than the found offset values.

If the accelerometer signals are reduced by the listed offset values, the reconstituted liquid force varies rather arbitrarily, with magnitude less than 0.001 N. The accelerometer data used in the sequel have been corrected for constant bias but remain to be processed for other deviations.



7 The liquid interaction with the tank

From the output of the MSS, properly corrected for errors, the force exerted by the water on the tank can be determined. An accelerometer with seismic point at location \mathbf{R} and with sensitive direction \mathbf{s} provides a nominal signal p [8]:

$$p = \mathbf{s} \cdot \boldsymbol{\sigma}(\mathbf{R}) = \mathbf{s} \cdot \boldsymbol{\sigma}(\mathbf{0}) + \mathbf{s} \cdot (\{\boldsymbol{\Omega}\}^2 + \{\boldsymbol{\Omega}'\})$$

or

$$p - \mathbf{s} \cdot \{\boldsymbol{\Omega}\}^2 \mathbf{R} = \mathbf{s} \cdot \boldsymbol{\sigma}(\mathbf{0}) - \mathbf{s} \cdot \{\mathbf{R}\} \boldsymbol{\Omega}' \quad (1)$$

With angular rate $\boldsymbol{\Omega}$ known from the gyro output each of the six accelerometers gives a different realisation of equation (1). These form a system of six linear equations for the components of the acceleration at the origin of the coordinate system $\boldsymbol{\sigma}(\mathbf{0})$ and the angular acceleration $\boldsymbol{\Omega}'$.

Solution of the system allows to determine the total force on the dry Sloshsat from:

$$\mathbf{F}_T = F_T \mathbf{e}_F = M_{\text{dry}} [\boldsymbol{\sigma}(\mathbf{0}) + (\{\boldsymbol{\Omega}\}^2 + \{\boldsymbol{\Omega}'\}) \mathbf{R}_M]$$

If the force from the thrusters is subtracted from \mathbf{F}_T , the force exerted by the water on the tank remains.

It is noted that the value of $\boldsymbol{\Omega}'$ needs to agree with its value as determined from the rate of change of the output of the gyroscopes, an item for MSS calibration. The force as determined from the uniform rotations in Table II is given in Table III.

Table III. Direction and magnitude of liquid force \mathbf{F}_T , and angle between \mathbf{F}_T and $\boldsymbol{\Omega}$, averaged over 2 minutes

Pass	eF(1)	eF(2)	eF(3)	F_T (N)	angle (°)
01	-0.2106	0.0413	0.9767	0.0905	88.9087
02	-0.1122	0.0833	0.9902	0.0789	88.9064
03	-0.9071	-0.2797	0.3145	0.0100	69.1902
04	-0.2103	0.0268	0.9773	0.1058	88.0454
05	-0.1537	0.0612	0.9862	0.1698	89.8320
06	-0.1422	0.0637	0.9878	0.2194	89.9788
07	-0.1192	0.0672	0.9906	3.2978	89.9198
08	-0.8869	-0.2424	0.3932	0.0101	75.6532
09	-0.9073	-0.3689	0.2019	0.0082	60.5408
10	0.7313	0.5621	0.3864	0.0011	61.2352



The force in Passes 03, 08, 09 and 10 is too small for a reliable determination of its direction. The remaining data correspond to a Weber number of 1.7 (Pass 02) or larger and therefore the inertial forces dominate, or, the centrifugal force must be about normal to the spin axis. The angle values show that the condition is closely met.

If one puts $\Omega' = \sigma(\mathbf{0}) = \mathbf{0}$ in equation (1), the system c.o.m. can be calculated as the system origin from a least-squares solution of the resulting equations. The values are in Table IV. Note that the c.o.m. directions are determined up to a component along the angular rate. However, comparison of the Y-values from Table IV with Figure 7 indicates that the unknown component is small at best. This is a consequence also from the fact that at maximum Z coordinate Y must be zero.

Table IV. C.o.m. locations from MSS output for sizable rotation rates of Table II.

Pass	system c.o.m. (x,y,z)			water c.o.m. (x,y,z)		
	01	0.0019	-0.0092	-0.1345	-0.0519	-0.0311
02	0.0123	-0.0091	-0.1390	-0.0119	-0.0306	0.0923
04	0.0022	-0.0092	-0.1331	-0.0508	-0.0308	0.1153
05	0.0078	-0.0091	-0.1338	-0.0291	-0.0307	0.1125
06	0.0086	-0.0089	-0.1326	-0.0261	-0.0299	0.1172
07	0.0103	-0.0088	-0.1297	-0.0195	-0.0294	0.1283

The aberrant value for Pass 02 is to be investigated.

Neither the dry tank nor the liquid mass configuration rotate about one of their principal axes and so there will be a (static) interaction torque. Its value is $\{\Omega; \underline{J}\Omega$, or $O(0.02 \text{ N.m})$ in Pass 07, and when it is sufficiently large to be identified by the MSS data, and larger than the leakage torque, remains to be analysed.

8 Sloshsat dynamic state

A large manoeuvre followed by over two hours of no thruster activation occurred in Pass 04. The Sloshsat rate is given in Figure 6; the reconstituted direction of the force on the tank is in Figure 7. Multiplied by 0.123 m, the average maximum distance of the water c.o.m. from the tank centre, the same should give a fair estimate of the trajectory of the water c.o.m. in the tank, and is given as an X-Y, X-Z plot in Figure 8.

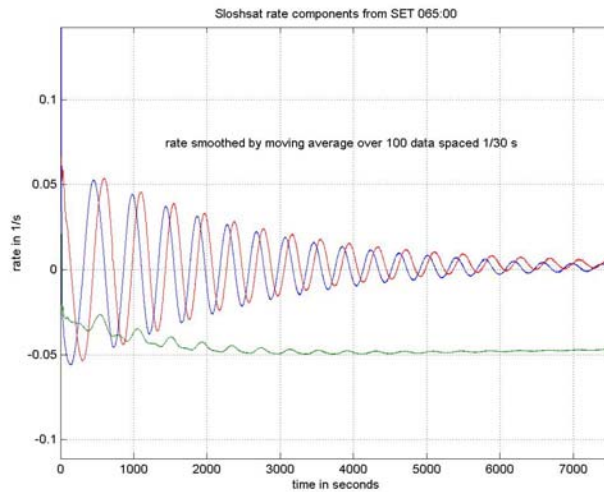


Figure 6 Sloshsat rate components from SET 065. The decrease of the Y-component magnitude after 5000 s warrants investigation.

The trajectory during large manoeuvres often starts out circular, then becomes linear and finally has a figure 8 shape. Figure 8 illustrates the latter (green curve), as does the blue (X) component in Figure 7.

In general the X, Y and Z components of vector quantities are shown blue, green and red respectively (Matlab convention); otherwise where noted.

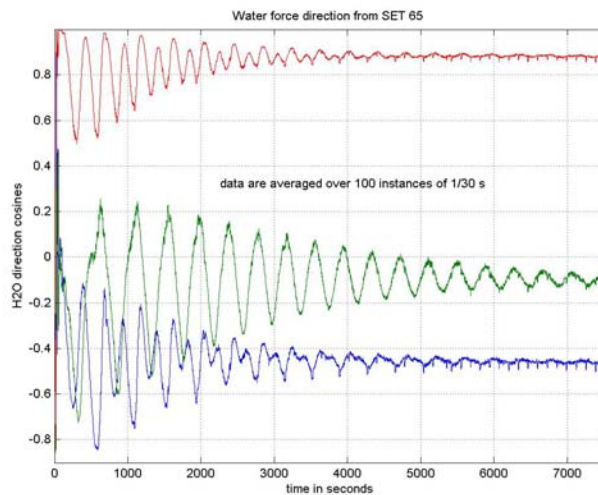


Figure 7 The liquid force direction.

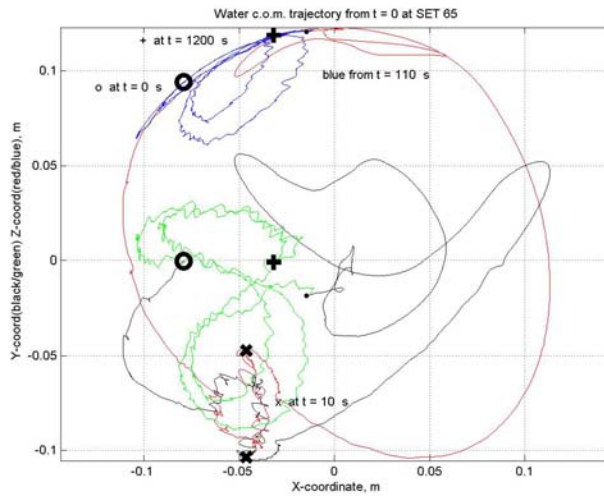


Figure 8 Approximate liquid c.o.m. trajectory.

The early development of the (raw) angular rate is shown in Figure 9, together with a prediction, the thin line graph, from the Sloshsat Motion Simulator (SMS).

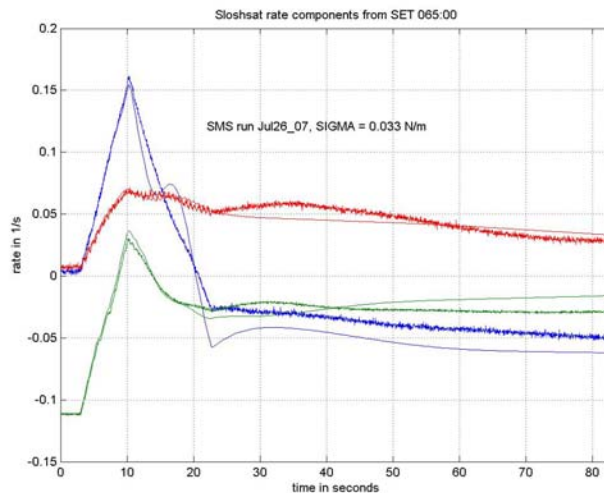


Figure 9 Initial Sloshsat rate and SMS prediction.

The simulation was run with the thruster commands as obtained from the Sloshsat telemetry. The beginning (at ~ 3 s) and end (at ~ 23 s) of the thruster activation period are clearly discernible. The deviation between observed and predicted rate components is reflected also in differences between predicted and observed liquid c.o.m. trajectories.



9 The Sloshsat Motion Simulator

A model for a spacecraft with a partially filled tank has been developed in support of the Sloshsat mission [9]. The liquid is modelled as a spherical mass, the 'slug', with variable size but constant density. Its size is controlled by the contact force between the slug and the tank wall, a function of the acceleration of the tank, the slug angular rate, surface tension and friction. From conservation of mass and momentum in the slug:

$$N - N_0 = m \left[\frac{3}{8} \{ r [\mathbf{e} \cdot \mathbf{x} (\boldsymbol{\Omega} + \boldsymbol{\omega})]^2 - \mathbf{e} \cdot (d\mathbf{V}/dt) \} + \frac{1}{4} (a - r) (\boldsymbol{\Omega} + \boldsymbol{\omega})^2 \right] - 5\pi\sigma(a - r) - f\dot{r} \quad (2)$$

where it is assumed that the normal force is along \mathbf{e} and $f\dot{r}$ is the friction related to the radial rate \dot{r} .

The slug exchanges momentum with the tank via the normal force, a friction force and a friction torque. The functional form and parameter values of friction are (to be) established from comparisons of measured data of liquid action with results from simulations by SMS. Such measured data are now taken from the literature; an example is given in the next section.

The slug is given a minimum size and thus a minimum moment of inertia. If this size is reached, the remaining radial rate is nullified via an impact with the tank wall. The restitution factor of the impact has been taken to decrease with the impact velocity.

The tank shape is modelled a sphere, but with an attractive force to the extreme X-locations. Such force is derived from the capillary potential Γ_0 in the free liquid surface; the area is minimal with all liquid at an end of the Sloshsat tank. The value of the potential is related to the difference in minimum and maximum free surface area, and was confirmed with simulated values of capillary stability [10]. For large Weber number, the capillary potential is no longer relevant but a same construct is used to model the effect on liquid flow from the elongated Sloshsat tank shape as compared to the spherical shape in SMS.

For 1.5 rpm SMS predicts the slug centre location at $[-0.046; 0.007; 0.116]$ m, to be compared with the values in Table IV (with the rather uncertain but small Y coordinate value). It did not change much for a potential value $\Gamma = 25 \Gamma_0$. However, for manoeuvres, such increase of potential has a large effect on the initial trajectory of the slug in the tank and, at several occasions, needed a good choice to achieve the same orientation (+ or -) of the final system rotation rate as was observed from Sloshsat.

The simulations for the manoeuvres in the present document showed a minimum size slug, i.e. no significant slug breathing motion was predicted. By changing the expression for capillary pressure, e.g. by a change of the surface tension value, breathing motion can be predicted more readily. An example (a change of sign) is mentioned later.

10 Sloshsat/SMS flat-spin manoeuvre

Starting at SET 112:31 in Pass 07, Sloshsat was taken to a rotation about its intermediate axis of inertia which is near the X-axis. Then control was stopped and, being in an unstable state, the spacecraft went back to a stable rotation about its major axis (near Y).

The inertial properties of Sloshsat are such that the equilibrium liquid c.o.m. is at nearly the same location for uniform rotation about the intermediate or about the major axis of inertia. The control, denoted CONTR11, commands the rotation about the average liquid c.o.m. location in order not to induce large liquid velocities in the transfer from initial (major) to final (intermediate) axis rotation. The manoeuvre requires a thrust force in addition to a torque and, from the limited thruster yield, the intended manoeuvre can be done only at a rotation rate of about 2 rpm. The transfer to the intermediate axis is followed by a spin-up to the desired rotation rate value, here about 4 rpm. This part of the manoeuvre is executed by a closed-loop PI control law, CONTR10.

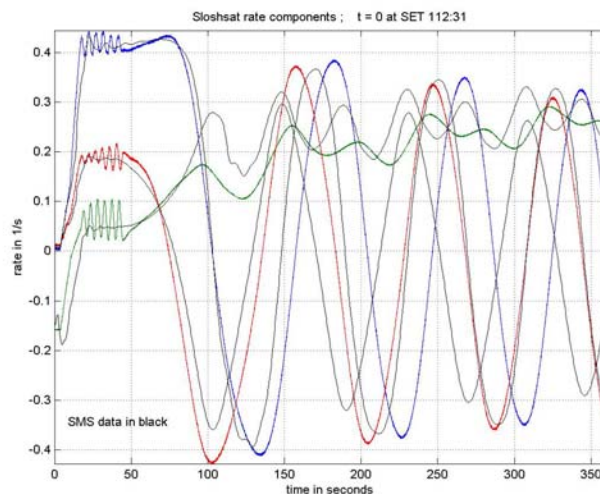


Figure 10 Sloshsat and SMS rate components. Control acts during about 40 s.

Although the thruster commands are available from telemetry, it was considered better to operate SMS also under the CONTR11/10 algorithms in order to get a close simulation of the commanded Sloshsat conditions at the termination of control. The actual and simulated early rates are shown in Figure 10. The simulation started with $\Gamma = 20 \Gamma_0$, to decrease linearly over 120 s to Γ_0 . This rate is not very critical and was chosen to achieve a gradual, rather than an abrupt, change back to Γ_0 . The large initial value of Γ causes a slug velocity of about 0.08 m/s after 3 s.

A remarkable feature is the growing amplitude of the Sloshsat rate Z-component (red) during CONTR10 activity, to be investigated in detail.

For the whole manoeuvre the red curve sinks deeper than the blue, but the blue curve peaks higher than the red, a shift not shown by the SMS prediction and likely related to different predictions also of other variables. For example consider the trajectory of the water c.o.m. Starting at 360 s, the trajectories are both closed in 70 s, but the predicted one is shorter and of different shape; see Figure 11 (for the normal force magnitude see the early part of Figure 13). From 60 s on, i.e. 300 s earlier, a similar picture appears (except that the trajectories are much more irregular) and the shape difference shows up in the departure of the predicted (black) rate component from the measurement at 90 s.

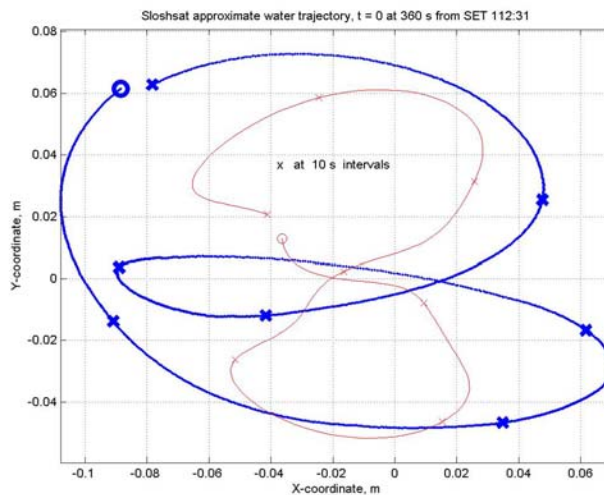


Figure 11 Two direction cosines of the Sloshsat normal force multiplied by 0.123 m, and the SMS prediction of the slug centre trajectory (thin red line).

For later times the (blue) Sloshsat trajectory remains similar but with a decreasing central loop and finally transcends to an elliptical shape. It is noted that the red 8-shape might change to the blue form for a larger slug attraction to the X poles. The predictions of later rate components with the data from Sloshsat are in Figure 12; the SMS curve frequency is about 5% low.

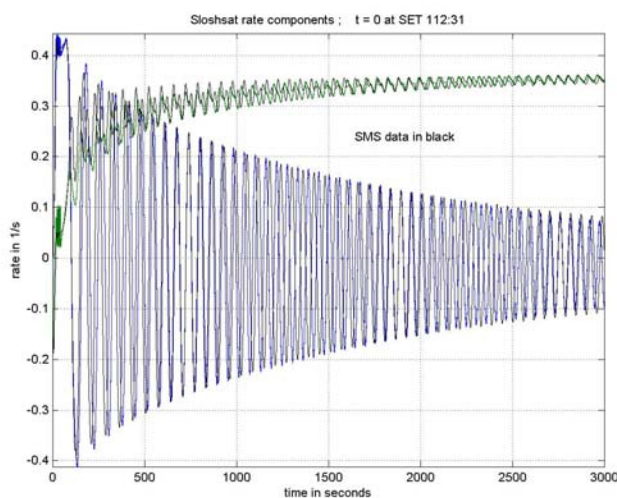


Figure 12 The late development of two (for clarity) rate components from figure 10.



The friction torque magnitude T_f between tank and slug in SMS has been based on the data in [11]; in formula:

$$T_f = 15 v_{mL} \omega \omega_0 / (\omega_0 - \omega) \text{ N.m} \quad (3)$$

ω_0 is the value of 1.08ω at the start of the manoeuvre.

In order to deal with the singularity $\omega = \omega_0$, a reset of ω_0 to 1.08ω is performed when ω reaches $0.926\omega_0$. Such may occur during (liquid) spin-over and -up when the slug relative rate grows larger than its initial value. The torque is taken along the direction of ω ; not much change came from simulations with an offset. The friction torque does not affect strongly the later nutation damping (see below) but influences the early development of the motion, after the thrusting.

The (sliding) friction force has been taken to act at the centre of the liquid slug, counter to the relative velocity of the slug in the tank. It reduces the liquid swirl.

$$\mathbf{F}_f = c_f m_L v / a^2 \mathbf{u} \text{ N} \quad (4)$$

Coefficient c_f was taken 4000, which is an order of magnitude larger than as would follow from a related expression in [12]. The Reynolds number for Sloshsat is much larger than in that analysis. The torque from \mathbf{F}_f is $O(R_M.F_f)$ generally larger than T_f and from about $t = 150$ s on, even an order of magnitude.

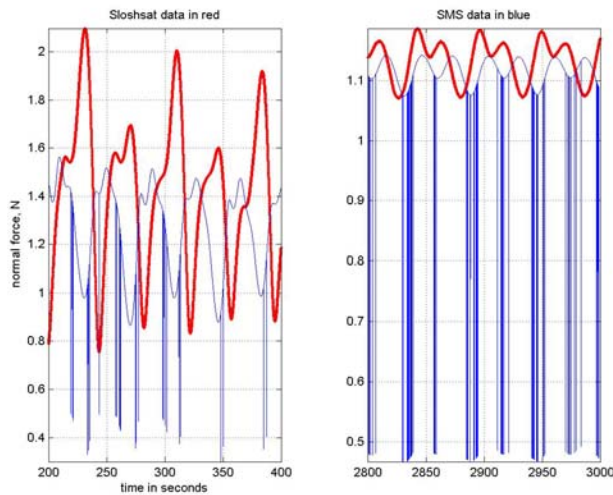


Figure 13 The normal force magnitude at times as in Figure 12. The spikes (blue) drop to the low value for a slug not at minimum size (or 'frozen').

The normal force at early and late periods is plotted in Figure 13. The predicted low value is near the Sloshsat result, but the predicted high value (that occurs at the crossing in the Figure 8



trajectory) is rather less than measured. It will bring a (slightly) different torque on the tank, which may affect the nutation frequency.

If the sliding friction is reduced strongly, one observes:

- slug swirl and normal force are increased.
- early oscillations of similar frequency as by Sloshsat during the CONTR10 period.
- some change in the detailed shape of the predicted Figure 8 slug trajectory.
- the nutation damping becomes considerably less than observed.
- a harmonious interaction develops between liquid swirl and tank rate.

For $c_f = 400$, and a five-fold increase of viscosity (i.e. F_f reduced by half, T_f increased by a factor five), SMS showed insufficient nutation damping and the normal force value was not improved significantly. A reversal of the sign of σ , that tends to enlarge the slug size, gave a single breathing early in the manoeuvre (together with a much reduced slug trajectory) and removed the spikes on the normal force magnitude.

SMS sliding friction now has been given such magnitude as to achieve the observed nutation damping of Sloshsat. It is stressed that this action occurs at low relative slug (liquid) velocities and should therefore be reviewed when Sloshsat data for low Weber number scenarios have been analysed.

Additional damping might be obtained through various displacements that cause work, e.g. via contact line stiction or via the forcing torque of the (rotating) liquid configuration. Slug impact has been mentioned already as a cause of kinetic energy loss.

11 Conclusions

Based on MSS data that have been corrected only for bias on the accelerometer signals, and for relatively large rotation rates the following has been concluded,

On the Sloshsat mission:

- precise calibration promises to lead to high resolution of significant forces from various physical phenomena.
- no sign of tank leakage as a cause of the major anomaly of the mission is seen.
- the real-time data distribution system FACT worked fine.
- detailed analysis of a large manoeuvre indicates that a flight mechanics model can become a valid and useful tool for slosh control on spacecraft.



On the performance of SMS:

- the predicted time histories of variables have signatures that are typically shown also by the measured data. Then, predictions of variables that cannot be measured should be valid.
- introduction of a potential force field in the tank allows achieving a fit between predicted and actual behaviour. The Weber number dependence of the potential is to be analysed, as is the effect of other variables.
- mechanisms for damping are to be reviewed and modelled anew, following evaluation of low Weber number data.

The tank instrumentation data are sorely missed; these were to have provided the clues for the improvement of the system model. The strategy now is to await predictions of liquid behaviour by CFD calculations of liquid c.o.m. trajectory and forces (e.g. from liquid 'kneading').

Nomenclature

Vector quantities have bold characters; the non-bold form represents the magnitude of the vector.

a	characteristic dimension of the tank 0.228 m
c.o.m	centre of mass
c_f	sliding friction coefficient
F_f	sliding friction force, N
<u>J</u>	dry Sloshsat inertia tensor, kg.m ²
m_L	liquid mass = 33.5 kg
M_{dry}	Sloshsat dry mass = 95.63 kg
N	Ne = liquid normal force, N
r	re = water c.o.m. location, m
R_M	dry Sloshsat c.o.m. at (0.0208, -0.0016, -0.2201)
T_f	liquid friction torque magnitude, N.m
u	slug relative velocity in the tank, m/s
$d\mathbf{V}/dt$	dry Sloshsat acceleration, m/s ²
We	rotational Weber number = $\rho \Omega^2 a^3 / \sigma$



Special symbols

O	order of magnitude
$\{ \mathbf{v} \} = \begin{bmatrix} 0 & -v(3) & v(2) \\ v(3) & 0 & -v(1) \\ -v(2) & v(1) & 0 \end{bmatrix}$	skew-symmetric matrix of vector \mathbf{v} , $\{ \mathbf{v} \} \mathbf{r} = \mathbf{v} \times \mathbf{r}$

Greek symbols

ν	water kinematic viscosity = $10^{-6} \text{ m}^2/\text{s}$
ω	liquid slug relative rotation rate, 1/s
Ω	tank rotation rate 1/s, Ω = magnitude
Ω'	tank angular acceleration, $1/\text{s}^2$
ρ	liquid density, for water = 1000 kg/m^3
σ	surface tension, for water = 0.072 N/m
Γ	tank potential, Γ_0 = capillary value, N.m
$\sigma(\mathbf{R})$	acceleration at \mathbf{R} , m/s^2

Acknowledgement

The first version of SMS has been coded in Fortran by Roel Mans.

Sloshsat FLEVO is a harmonised programme between the European Space Agency (ESA) and the Netherlands Agency for Aerospace Programs (NIVR). Main contractor is the National Aerospace Laboratory NLR (The Netherlands), with participation of Fokker Space (The Netherlands), Verhaert (Belgium), Rafael (Israel) and NASA (USA).

The Sloshsat FLEVO development is performed in the framework of the ESA Technology Demonstration Programme (TDP) Phase 2 and the NIVR Research and Technology (NRT) programme.

The Sloshsat data are Copyright ESA and NLR, 2005.



References

- [1] J.P.B. Vreeburg and A.E.P. Veldman. "Transient and sloshing motions in an unsupported container" in *Physics of fluids in microgravity*, R. Monti, Ed. , London: Taylor & Francis, pp. 293-321, 2001.
- [2] F.T. Dodge and D.D. Kana. "Liquid slosh dynamics and control technology program" AIAA paper 91-3547, presented at the Conference on Advanced SEI Technology, Cleveland, OH, 4-6 September 1991.
- [3] J.J.M. Prins. "Sloshsat FLEVO project, flight, and lessons learned" paper IAC-05-B5.3./B5.5.05, 2005
- [4] J.P.B. Vreeburg and D. Soo (eds.) Colloquium on Sloshsat and Liquid Dynamics in Spacecraft. Estec, Noordwijk, NL 16-17 November 1998. ESA WPP 158.
- [5] S. Adler, A. Warshavsky and A. Peretz. "Low-Cost Cold-Gas Reaction Control System for Sloshsat FLEVO Small Satellite" *Journal of Spacecraft and Rockets*. Vol. 42, no. 2, pp. 345-351. Mar.-Apr. 2005
- [6] J.P.B. Vreeburg. Sloshsat FLEVO Experiment Definition Document (EDD), Flight Issue (draft) SLOSHSAT-NLR-CD-02. October 2004.
- [7] R. Luppés, J.A. Helder and A.E.P. Veldman, "Liquid Sloshing in Microgravity", paper IAC-05-A2.2.07, 2005. Also: <http://www.math.rug.nl/~veldman/>
- [8] J.P.B. Vreeburg. "Identification of the geometry of accelerometers in an arrangement" *Acta Astronautica*, Vol 48, Nos 5-12, pp 479-483, 2001.
- [9] J.P.B. Vreeburg. "Dynamics and control of a spacecraft with a moving, pulsating ball in a spherical cavity" *Acta Astronautica*, Vol 40, Nos 2-8, pp 257-274, January-April 1997.
- [10] J.P.B. Vreeburg and D.J. Chato. "Models for liquid impact onboard Sloshsat FLEVO" AIAA paper 2000-5152, presented at the AIAA Space 2000 Conference, Long Beach, CA, 19-21 September 2000.
- [11] K. Michaelidis. "Reibungsmomente der instationären Bremsströmung am Zylindermantel eines flüssigkeitsgefüllten zylindrischen Gefasses" *Acta Mechanica*, Vol 26, pp 1-13, 1977.
- [12] P.G. Bhuta and R.L. Koval, "A viscous ring damper for a freely precessing satellite" *Intern Journal of Mechanical Science*, Vol 8, pp.383-395, 1966.